Environ. Water Eng., 2025, 11(3), 305-315 https://doi.org/10.22034/ewe.2025.498706.1995

EWE

Environment and Water Engineering

Homepage: www.jewe.ir

ISSN: 2476-3683

Sesame-residue biochar as a sorbent for salinity ions: capacity, isotherm, and kinetics

Mohammadreza Nouri-Shamsi[1], Somayeh Soltani-Gerdefaramarzi[1,2]✉, Mohsen Ghasemi[3], and Najmeh Yarami[1]

[1]Department of Water Sciences and Engineering, College of Agriculture and Natural Resources, Ardakan University, Ardakan, Iran

[2]Member of Water, Energy and Environment Research Institute, Ardakan University, Ardakan, Iran

[3]Regional Water Company of Yazd, Ministry of Energy, Yazd, Iran

ARTICLE INFO

Paper Type: Research Paper

Received: 09 January 2025
Revised: 10 February 2025
Accepted: 07 April 2025
Published: 19 April 2025

Keywords
BET
Biochar
Desalination
Langmuir
Saline Wastewater

Corresponding author:
S. Soltani-Gerdefaramarzi
✉ ssoltani@ardakan.ac.ir

ABSTRACT

Water scarcity is a reality in arid and semi-arid regions, leading to competition for limited water resources among agricultural, domestic, and industrial needs. In this study, sesame seed residue (Sr) adsorbents and biochar produced at 400 (B1), 500 (B2), and 600 °C (B3) were used to remove salt ions from agricultural saline wastewater. Fourier transform infrared spectroscopy (FTIR), X-ray diffraction (XRD) patterns, and Brunauer-Emmett-Teller (BET) theory were used to determine the different properties of the adsorbents. Four adsorbent treatments were batch tested at salinity levels of 5, 10, 20, and 35 dS/m in three replicates. Ion concentrations of Na^+, Ca^{2+}, Mg^{2+}, Cl^-, SO_4^{2-}, and HCO_3^- and primary and secondary EC before and after adsorption were measured. Various parameters, such as contact time, initial concentration of salt ions in the water, and isotherm and adsorption kinetics, were investigated. The results showed that in the four salinity levels of 5, 10, 20, and 35 dS/m, the maximum value of solute adsorption was 24.4, 57.0, 139.9, and 308.6 mg/g for adsorbent B3, respectively. The largest and smallest decreases in saline water EC occurred for B3 and Sr at salinity levels of 35 and 5 dS/m, respectively, which reduced the water salinity by approximately 31 and 3%, respectively. While low-cost adsorbents derived from agricultural waste are capable of adsorbing salt or removing contaminants from aquatic environments, they also have limitations that have led to ongoing research.

Highlights

- Increasing the pyrolysis temperature raised the adsorbent surface area and adsorption capacity.
- K+ and Cl- were the least and most absorbed ions, respectively, at all salinity levels.
- The pseudo-second-order and Langmuir models best described adsorption kinetics and isotherms.

Citing:
Nouri-Shamsi, M., Soltani-Gerdefaramarzi, S., Ghasemi, M., & Yarami, N. (2025). Sesame-residue biochar as a sorbent for salinity ions: capacity, isotherm, and kinetics. *Environment and Water Engineering*, *11*(3), 305-315. https://doi.org/10.22034/ewe.2025.498706.1995

1. Introduction

Treatment and reuse of wastewater and reclaimed water are being considered as new sources to compensate for some of the deficiencies in the agricultural and industrial sectors due to the increase in world population, lack of water resources, lack of rainfall, and environmental concerns (Lin et al., 2017). The use of treated wastewater has always been a subject of attention and investigation in many countries worldwide. In most developed countries, treated wastewater is used for various applications based on relevant standards. These applications include agricultural irrigation, water supply for industries, and even use in public applications such as watering parks and gardens. The use of treated wastewater not only helps reduce the consumption of freshwater resources but also contributes to environmental protection and pollution reduction (Chen et al., 2023). Many countries, especially in arid and water-scarce regions, are implementing advanced treatment systems to utilize these resources, given the increasing need for water. Therefore, the development of new technologies in the field of wastewater treatment and the improvement of treated water quality have become a fundamental priority for many countries. Consequently, this approach is considered a sustainable solution to the challenges related to water resource management, water supply, and

environmental protection, and it can have positive impacts on society and the economy (Ghasemi et al., 2017). On the other hand, desalination of salt water is one of the most important issues in the world today. The pressure on groundwater resources and the consequences of over-exploitation of water resources can be minimized by using drain sewage as an alternative source of water for irrigation (Ghasemi et al., 2018). It should be noted that agricultural drainage water cannot be used directly as irrigation water due to its excessive salt content. Therefore, it is necessary to purify agricultural drainage water before use (Aghakhani et al., 2011; Rostamian et al., 2015). Various methods have been invented to desalinate salt water, including reverse osmosis, electrodialysis, evaporation, and surface adsorption using adsorbents. The use of inexpensive absorbents is unavoidable in the reduction of water salinity due to the relatively high cost of these methods. In reverse osmosis and electrodialysis, although high efficiency and lack of importance of the effect of pH and temperature on the efficiency of pollutant removal are among the advantages of this method, high cost and lack of flexibility with pressure changes are among the disadvantages of these methods. Although the biological method has an efficiency of more than 99 percent and is environmentally friendly, the need to dispose of waste and the effect of temperature can be considered among its disadvantages (Hasan-Abadi et al., 2024). So far, the removal of salt ions from aqueous solutions has been the subject of the use of various adsorbents (Priya et al., 2020; Li et al., 2022).

Biochar is one of the most widely used adsorbents for water desalination due to its special morphology and suitable properties. These adsorbents generally can bind with the saline ions and cause the water to desalinate (Chen et al., 2023). Biochar is a carbon material with a high specific surface area and high porosity, which has become one of the industrial adsorbents due to its high adsorption capacity (Yang et al., 2020; Jellali et al., 2021). Agricultural and plant residues are suitable materials for biochar production. The main materials used to produce biochar include coal, charcoal, pine cones, coconut shells, almond shells, hazelnut shells, pistachio shells, walnut shells, slag, sugarcane bagasse, and waste containing carbon from sewage (Qiu et al., 2022). Agricultural activities can be developed in arid and semi-arid areas if it is possible to convert agricultural residues into suitable adsorbents for water purification (Younis et al., 2020; Luo et al., 2022). Sahraei et al. (2022) investigated the use of Iranian zeolite and bentonite as mineral adsorbents in desalination. Their results showed that these two adsorbents did not have the necessary efficiency to reduce salinity and caused an increase in the electrical conductivity and sodium content of the water. However, their efficiency increased after modification with acid. Hoveizavi et al. (2024) investigated the reduction of agricultural drainage salinity using coco peat as an adsorbent and concluded that coco peat has the potential to reduce the electrical conductivity of saline water by approximately 20%. Hasan-Abadi et al. (2024) investigated the efficiency of biochar for desalination in the presence of copper ions. Their results showed that biochar derived from sesame meal exhibited desirable performance in desalinating saline wastewater containing copper ions via adsorption, due to its high active surface area, porous structure, and suitable surface functional groups. Based on the review of sources, it is clear that previous studies have focused more on the use of biochar adsorbents to remove heavy metals from aquatic environments, and less attention has been paid to the use of these products in desalination. However, the great capacity of these adsorbents to absorb salinity factor ions such as Na^+ and Cl^- has been demonstrated by some studies in this field (Shokrian et al., 2017 and 2020; Hasan-Abadi et al., 2024).

Although some studies have been conducted, the potential of using sesame residue biochar as a salt ions absorber from aqueous solutions has not been investigated. Inexpensive adsorbents derived from agricultural waste can adsorb salt or remove contaminants from aquatic environments, however, they also have limitations that have led to continued research. Considering that the absorbent material should be both readily accessible and cost-effective, sesame residues are abundantly available in Ardakan city, Iran due to the local production of sesame-derived products, and they can be obtained at a reasonable price. The purpose of this study was to prepare biochar from sesame residues, investigate the effect of carbonization temperature on its properties, and evaluate the desalination potential of biochar prepared by pretreating agricultural saline water.

2. Materials and Methods

The adsorption of salt ions was evaluated in a batch experiment. The Freundlich and Langmuir models were applied to investigate the adsorption isotherm, and the Intra-particle diffusion, pseudo-first-order, and pseudo-second-order models were also used for kinetic studies. To prepare the saline water and to match the natural conditions with the laboratory conditions, the required saline water was collected from the drains of Chah-Afzal Ardakan area with 32.5° N; 53.8° E; and approximately 750 m elevation, about 90 km north of Yazd city in Iran with a salinity of about 35 dS/m and by diluting the saltwater sample, salinity levels of 5, 10, and 20 dS/m were prepared for further experiments. Ion concentrations of Na^+, Ca^{2+}, Mg^{2+}, Cl^-, SO_4^{2-}, and HCO_3^- at various EC levels are shown in Table 1.

According to Table 1, among the anions in water samples with an EC of 35 dS/m, Cl^- is the most abundant anion in aqueous solution, accounting for 44.1% of the total ions in water. The amount of Cl^- in the aqueous solution is approximately 10 times greater than the amount of HCO_3^- ions in the water and 2.8 times greater than the amount of SO_4^{2-} ions in the saltwater solution. Among the cations in the saltwater sample, Na^+ is also the most abundant cation in the water, accounting for 29.8% of the total ions dissolved in the water. The amount of Na^+ in water is about 37 times that of K^+ in water, 13 times that of Ca^{2+}, and 11 times that of Mg^{2+} ions in water. This causes Na^+ and Cl^- to become the dominant ions in the saltwater. Data analysis and comparison of means were performed using SPSS version 24 software. The Least Significant Difference (LSD) test was performed at the 5% level to compare the means of the treatments.

Table 1 Concentration of cations and anions in saline water used for experiments

(dS/m) EC	pH	TDS	K^+	Na^+	Ca^{2+}	Mg^{2+}	Cl^-	HCO_3^-	SO_4^{2-}
		(mg/l)							
5	8.6	3071.8	48.2	814.3	53.3	134.1	1240	299.5	482.4
10	8.6	6118.3	75.1	1654.4	125.9	255.2	2589.9	448.3	969.5
20	8.5	12213	131.8	3526.2	257.1	388.6	5318.1	622.8	1968.4
35	8.5	21338.3	171.3	6356.8	488.2	577.2	9407.9	944.1	3392.8

2.1 Preparation of adsorbents

Sesame residue (Sr) used in this research was prepared from the center of sesame products located in Ardakan city, Iran. To prepare the Sr, the sesame residues were first washed well with distilled water. Then they were dried in the room for 48 hours and then placed in an oven at 105 °C for 24 hrs to remove the rest of the moisture. They were then ground and separated by standard sieves of particles between 0.5 and 1 mm for use in this research. Prepared Sr was placed in an electric furnace under inert nitrogen gas and the temperature of the furnace was increased at a rate of 10°C/min to 400 °C to prepare biochar as an adsorbent treatment. Then, it was kept at 400 °C for 120 min to pyrolyze the sesame residue well. Then, nitrogen gas was applied to bring the furnace temperature to the ambient temperature (B1). In the same way, the biochar was also produced at the temperature of 500 (B2) and 600 (B3) °C (Li et al., 2022). Table 2 shows some physical and chemical properties of the adsorbent used in this study.

Table 2 Some adsorbent physical and chemical properties

Property	Sr	B1	B2	B3
Specific weight (g/cm^3)	0.187	0.387	0.417	0.478
Specific area (m^2/g)	73.21	198.43	238.17	317.21
Average diameter of holes (nm)	3.18	2.53	2.24	1.87
Hole volume (cm^3/g)	0.043	0.101	0.123	0.168
Production efficiency (%)	-	48.19	41.98	37.85
Ash (%)	-	18.46	20.21	23.13
pH	7.35	8.01	8.22	8.3
EC (dS/m) in water	0.24	0.17	0.16	0.16

Sr, Sesame residue; B1, Biochar-400; B2, Biochar-500; B3, Biochar-600

2.2 Instrumentation

Fourier transform infrared spectroscopy (FTIR) was used to identify and study the type of functional groups effective in the adsorption of each adsorbent and to justify their adsorption characteristics and differences. For this purpose, the Shimadzu IR Prestige-21 in the 400-4000 cm^{-1} range using the KBr tablet method was used. To determine the crystal structure and phase, X-ray diffraction (XRD) patterns of the adsorbents were determined using a diffractometer (X'PERT MPD, Philips, Amsterdam, The Netherlands). Brunauer-Emmett-Teller (BET) theory was used to determine the surface areas of the adsorbents. This experiment was conducted using a Mini2-Belsorp device, Japan.

2.3 Batch adsorption experiments

The adsorption of salt ions from saline irrigation water was evaluated in batch experiments. These experiments were conducted at four salinity levels (5, 10, 25, and 35 dS/m) and with four adsorbent treatments (Sr, B1, B2, and B3) in 3 replications as a factorial experiment in a completely randomized design. One gram of each of the adsorbents was added to 50 ml of saltwater samples. The mixtures were shaken for 4 hrs at room temperature. 5B filter papers were then used to separate the adsorbents from the solutions. EC, pH, and ion concentration were determined using standard analytical methods before and after adsorption. Furthermore, the adsorption capacity (q_t, mg/g) and the percentage of ions adsorbed by the adsorbents (E) were also calculated using Eqs. 1 and 2.

$$q_t = \frac{(c_0 - c_t)\, v}{w} \quad (1)$$

$$E = \frac{(c_0 - c_t)}{c_0} * 100 \quad (2)$$

where C_0 and C_t (mg/l) = initial and final anion concentrations in the solution, respectively; V = volume of the solution (l); and W = used mass of the adsorbent (g).

2.4 Adsorption isotherms

Adsorption isotherm tests were performed to further investigate the effect of ion concentration on the adsorption process. Saline water with ECs of 5, 10, 15, and 25 dS/m was used, and isothermal tests were performed at 25 °C with an adsorbent dosage of 1 g/50 ml and a stirring speed of 180 rpm for the best adsorbent in adsorption experiments. Three adsorption isotherm models (Langmuir, the Freundlich, and the Temkin isotherm model) were used. These models are widely used to describe the correlation of data. In the Langmuir isotherm model (Eq. 3), the adsorption is assumed to be monolayer (Salehzadeh et al., 2024) whereas the heterogeneous surface energies are explained by the Freundlich isotherm model (Eq. 4) of multilayer adsorption (Fatholahi et al., 2023).

$$q_e = \frac{q_m k_l C_e}{1 + k_l C_e} \quad (3)$$

$$q_e = k_f C_e^{\frac{1}{n}} \quad (4)$$

$$q_e = B\, ln\, (A \times C_e) \quad (5)$$

where q_e is the amount of adsorbed component per unit mass of adsorbent at equilibrium (mg/g); q_m: adsorption capacity (mg/g); C_e: equilibrium concentration of adsorbent in the solution after adsorption (mg/l); K_l: Langmuir constant (L/mg); K_f and n: Freundlich constants related to adsorption capacity and intensity, respectively; A and B are the Temkin isotherm constant (Ahmed and Theydan, 2013).

2.5 Effects of contact time and adsorption kinetic study

The influence of the contact time on the amount of salt ions adsorbed has been studied at different points in time. The adsorption kinetic experiments were carried out at a salinity level of 35 dS/m for the best adsorbent at contact times 10, 30, 60, 120, 180, 300, and 1440 min. For this purpose, kinetic studies were performed at a temperature of 25 °C, an adsorption dose of 1 g/50 ml, a solution pH of 8.2, and a stirring speed of 180 rpm and then the ion adsorption kinetic data were fitted to the kinetic models pseudo-first-order kinetic model (Eq. 6; Lagergren, 1898), pseudo-second-order kinetic model (Eq. 7; Ho and McKay, 1999) and Intra-particle diffusion (Eq. 8; Simonin and Bouté, 2016) as follows:

$$L_n(q_e - q_t) = L_n q_e - K_1 t \quad (6)$$

$$\frac{t}{q_t} = \frac{1}{K_2 q_e^2} + \frac{t}{q_e} \quad (7)$$

$$q_t = K_i \times t^{0.5} + c \quad (8)$$

where K_1 (min^{-1}), K_2 (g/mg min), K_i (mg/g $min^{0.5}$), and c (mg/g) adsorption rate constants; and q_t amount of adsorbed component per unit mass of adsorbent at time t (mg/g).

3. Results and Discussion

3.1 Characteristics of absorbents

As shown in Table 2, the specific weight of Sr was 0.187 g/cm^3, which decreased to 0.487 g/cm^3 after being converted to B3 due to the reduced volume of the biochar. Additionally, the specific surface area of Sr was 21 m^2/g. This increased to 317.21 m^2/g after conversion to B3. In general, as the pyrolysis temperature of Sr has been raised, the amount of specific surface has also been raised, increasing the adsorption capacity. Results of BET analysis, adsorption, and desorption isotherm for B1, Biochar-400 are shown in Fig. 1a. The BJH (Barrett-Joyner-Halenda) analysis is a method used in conjunction with BET (Brunauer-Emmett-Teller) analysis to characterize the pore size distribution of porous materials, such as adsorbents. While the BET method primarily focuses on determining the surface area, BJH analysis provides insights into the porosity of the material, specifically the sizes of the pores (Fig. 1b).

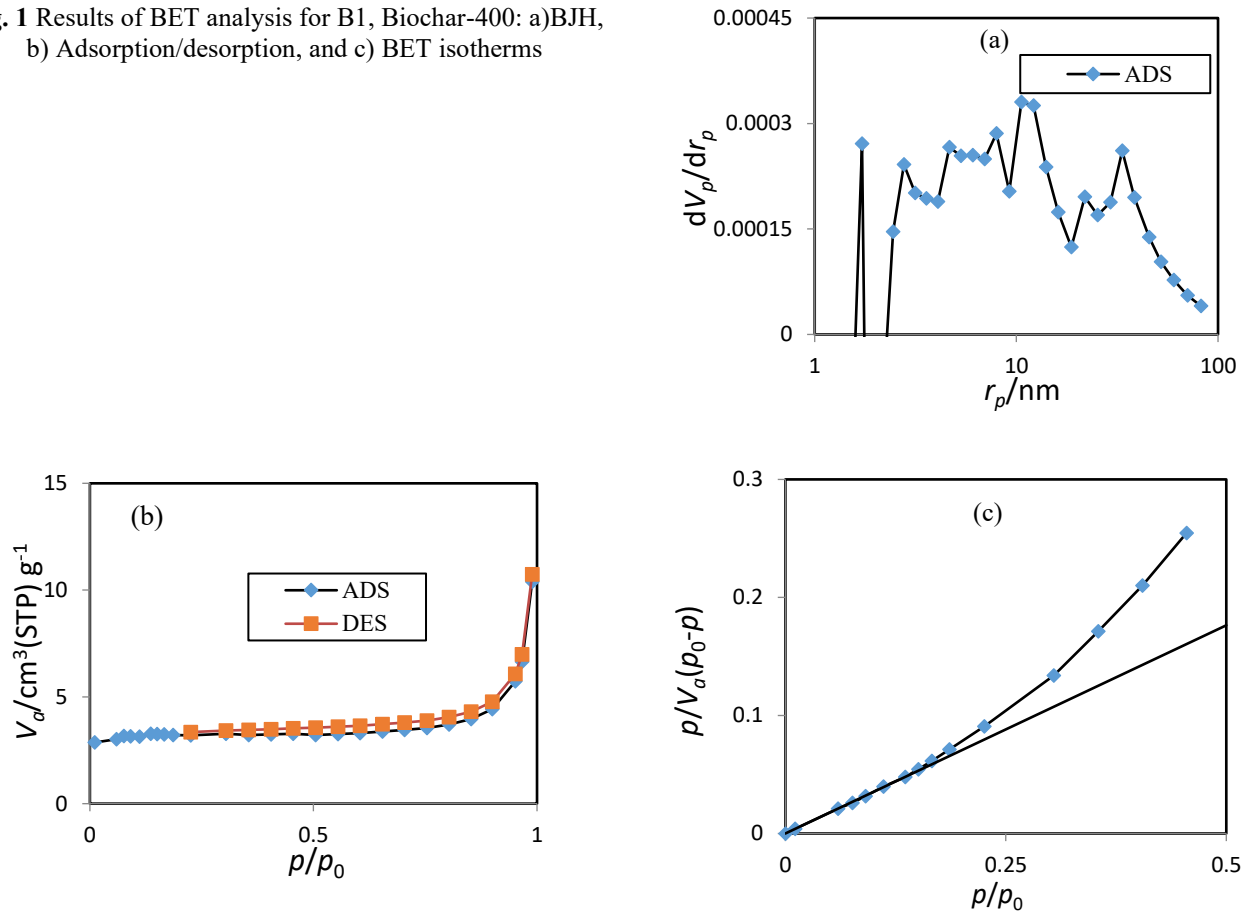

Fig. 1 Results of BET analysis for B1, Biochar-400: a)BJH, b) Adsorption/desorption, and c) BET isotherms

Based on the results of this analysis, the majority of pore volume appears to be concentrated in the 1 to 10 nanometer range, indicating the presence of mesopores. While a portion of the curve extends into the 10 to 100 nanometer range, likely, some macropores are also present, but the primary concentration is observed in the mesopore region. Figure 1c

shows the adsorption isotherm data collected by adsorbing a gas (commonly nitrogen) onto the surface of the material at a constant temperature, typically 77 °K. The data, as (P/P_0) values (the ratio of equilibrium pressure to saturation pressure) are obtained for various amounts of gas adsorbed. Min et al. (2011) reported that at low pyrolysis temperatures, the natural structure of the voids allows the release of gases resulting from the decomposition of the substrate without the need for a fundamental change in its morphological structure. On the other hand, at high pyrolysis temperatures, the production of a large volume of volatiles in a short time leads to increased porosity on the bed surface (Liang et al., 2021). The increase in porosity volume is also responsible for the decrease in hole diameter in B3 compared to Sr. The pH of Sr was 7.35, which reached 8.3 for biochar 600. Singh et al. (2010) reported that the pH of biochar increases with increasing pyrolysis temperature, which may be caused by the high presence of alkali metal salts such as sodium, potassium, calcium, and magnesium in biochar. The production efficiency of B2 is 48.19% and this rate was 37.85% for B3. This decrease in efficiency with increasing temperature could be due to the release of large amounts of volatile gases, which are easily released at high temperatures. In addition, the percentage of biochar ash production increased from 12.28 to 23.13% as the temperature of biochar production increased, the main reason being the greater oxidation of organic materials in the pyrolysis process at higher temperatures (Rodriguez-Reinoso et al., 1985).

Results of XRD patterns for B1, Biochar-400, are shown in Fig. 2. The presence of peaks in the 2θ range of 20 to 30 degrees can indicate specific crystalline properties that may impact the chemical and physical behavior of the material. Peaks in this range may indicate the presence of micro- and mesoporous characteristics in the material, which are vital for adsorption and separation applications.

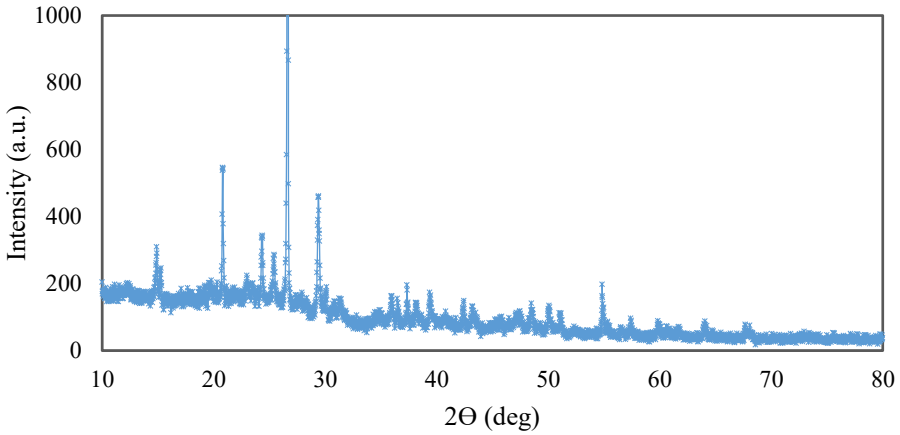

Fig. 2 X-ray diffraction patterns for B1, Biochar-400

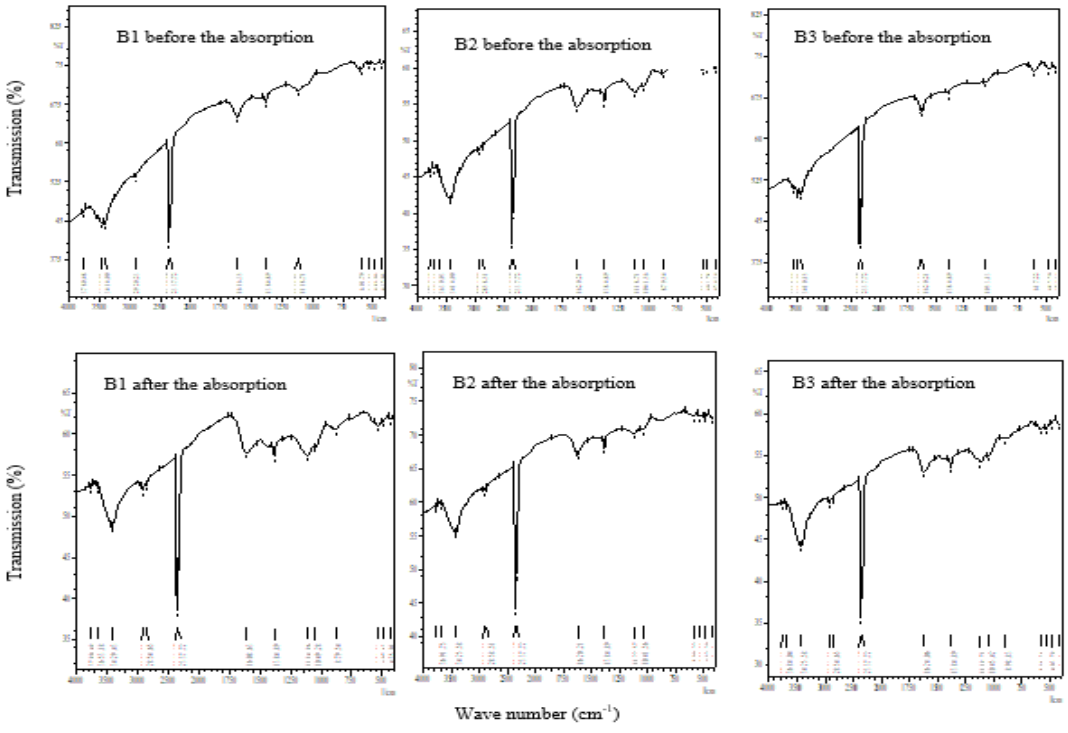

Fig. 3 Infrared spectra of absorbers in two states before and after the adsorption process

3.2 FTIR analysis

FTIR was used in this study to identify effective absorbing groups. Infrared spectra of absorbers in two states before and after the adsorption process in the wavelength range from 400 cm^{-1} to 4000 cm^{-1} are shown in Fig. 3. It shows that the intensity of some functional groups decreases with increasing carbonizing temperature. Hasan-Abadi et al. (2024) and Rostamian et al. (2015) also presented similar results. According to Figure 1, the peak shown in the spectrum of the 3410 cm^{-1} graph indicates the presence of free hydrogen or alcoholic OH groups in alcohols, phenols, and hydroxy-related carboxylic acids (Salehzadeh et al., 2024). After adsorption (Fig. 3), this peak reached 3425, 3429, and 3424 cm^{-1} for B1, B2, and B3, respectively. This shows the effect of this group of compounds on the adsorption of salt ions. Also, the peak located at the wavelength of 2918 cm^{-1} is related to the vibration of the stretching bond of aldehyde (Altintig et al., 2016). After adsorption, this peak shows the effect of this functional group in the adsorption of salt ions as it reaches 2920, 2921, and 2925 cm^{-1} for B1, B2, and B3, respectively. In addition, the peaks at the wavelengths of 1624, 1385, and 1040 cm^{-1} are associated with the C=O stretching band, C-H band, and C-O band, respectively, for rotational and non-rotational compounds (Ghasemi et al., 2018). The strong peak observed at the wavelength of 1045 cm^{-1} is related to the asymmetric stretching vibration of Al-O. After adsorption, this peak reaches 1049, 1041, and 1046 cm^{-1} for B1, B2, and B3, respectively (Doula, 2007). Finally, the peaks at wavelengths 890, 601, and 455 correspond to T-O and Si-O bands, O-T-O bands, and TO_4 internal bands, respectively. Based on the FTIR spectrum of biochar, we may say that carboxylic groups and aldehyde bonds play an important role in adsorption.

3.3 Desalination capacity by adsorbents

This section examined the ability of adsorbents at different salinities to adsorb salt-related ions, including K^+, Na^+, Ca^{2+}, Mg^{2+}, Cl^-, SO_4^{2-}, and HCO_3^-. Table 3 shows the amount of cations and anions absorbed by Sr and biochar produced from it at different salinities. According to the results, the highest adsorption of salinity factor ions is associated with B3 at a salinity level of 35 dS/m. In addition, Cl^- anion at 140.7 mg/g (approximately 2.7 times the capacity of Sr) and K^+ cation at 2.5 mg/g are the highest and lowest adsorption rates of B3 at a salinity of 35 dS/m. The amount of Cl^-absorbed by Sr, B1, B2, and B3 was 25.9, 42.6, 50.9, and 63.9 mg/g, respectively, at a salinity level of 20 dS/m (nearly half of the absorbed Cl^- is at a salinity of 35 dS/m). In addition, as the temperature of the production of biochar has increased, the amount of Cl adsorption has also increased significantly. Sr, B1, B2, and B3 adsorbents absorbed 31.9, 58.1, 72.6, and 95.5 mg/g of Na^+ cations, respectively. Thus, the amount of Na^+ adsorption was calculated to be almost 2.9 times higher when converting Sr to B3. Therefore, it was found that pyrolysis of sesame residue and its conversion into biochar also increased the adsorption of Na^+ ions dissolved in saline water. Na^+ adsorption also increased significantly with increasing salinity (Table 3). In general, it can be concluded that higher salinity adsorbents performed better in Na^+ adsorption than lower salinity adsorbents. Shokrian et al. (2017) evaluated the reduction of chlorine and sodium ions from salt water by rice husk and oyster biochar. Their results showed that the total adsorption percentage of chlorine and sodium ions for these absorbents was approximately 58%. Rostamian et al., (2015) and Ghasemi et al. (2017) and (2018) also investigated the use of different adsorbents to remove salinity from water and reported that among the ions responsible for salinity, the highest amount of adsorption is associated with chlorine and sodium ions.

Table 3 The amount of cations and anions absorbed (mg/g) at different salinity levels

Adsorbent	EC1 (dS/m)	K^+	Na^+	Ca^{2+}	Mg^{2+}	Cl^-	HCO_3^-	SO_4^{2-}	EC2 (dS/m)	EC Reduction %
Sr	5	0.1^{i}	1.6^{j}	-0.1^{i}	-0.05^{ij}	3.4^{l}	-0.2^{j}	0.9^{l}	4.83	3.4
B1	5	0.2^{hi}	2.8^{ij}	0.2^{hi}	0.5^{i}	5.0^{k}	1.0^{i}	1.7^{k}	4.69	6.2
B2	5	0.3^{h}	4.5^{i}	0.3^{hi}	0.7^{hi}	3.7^{l}	1.8^{hi}	2.8^{jk}	4.45	11.0
B3	5	0.3^{h}	6.0^{h}	0.4^{h}	0.8^{h}	10.6^{i}	2.4^{g}	3.8^{j}	4.30	14.0
Sr	10	0.2^{hi}	4.4^{i}	-0.2^{i}	-0.2^{j}	7.8^{j}	-0.4^{jk}	2.7^{jk}	9.52	4.8
B1	10	0.3^{h}	7.5^{gh}	0.5^{g}	1.3^{g}	12.8^{hi}	2.0^{h}	4.9^{i}	9.01	9.9
B2	10	0.5^{g}	9.4^{g}	$0.9f^{g}$	1.7^{f}	18.2^{h}	3.4^{fg}	6.3^{h}	8.71	12.9
B3	10	0.7^{f}	15.4^{f}	1.2^{f}	2.4^{e}	25.1^{g}	4.0^{f}	8.2^{g}	8.22	17.8
Sr	20	0.5^{g}	15.2^{f}	-0.5^{ij}	-0.4^{k}	25.9^{g}	-0.6^{k}	10.3^{f}	18.02	9.9
B1	20	1.0^{e}	24.6^{e}	1.8^{e}	2.7^{de}	42.6^{f}	4.7^{e}	13.7^{e}	16.72	16.4
B2	20	1.3^{d}	30.0^{de}	$2.1d^{e}$	2.9^{d}	50.9^{e}	4.7^{e}	16.7^{d}	16.02	19.9
B3	20	1.5^{c}	38.7^{d}	2.7^{d}	4.0^{c}	63.9^{d}	6.5^{d}	22.6^{c}	15.13	24.3
Sr	35	0.8^{ef}	31.9^{de}	-0.7^{j}	-0.5^{k}	52.0^{e}	-2.4^{l}	15.5^{de}	30.78	12.0
B1	35	1.4^{cd}	58.1^{c}	4.3^{c}	4.8^{bc}	95.1^{c}	7.6^{c}	31.1^{bc}	27.49	21.4
B2	35	1.7^{b}	72.6^{b}	5.2^{b}	6.2^{b}	108.8^{b}	9.1^{b}	36.0^{b}	26.21	25.1
B3	35	2.5^{a}	91.5^{a}	7.3^{a}	8.2^{a}	140.7^{a}	13.5^{a}	44.9^{a}	24.09	31.2

At the 5% probability level, the numbers sharing a common letter in each column are not significantly different according to the LSD's test; Sr, Sesame residue; B1, Biochar-400; B2, Biochar-500; B3, Biochar-600.

The SO_4^{2-} adsorption of Sr, B1, B2, and B3 adsorbents is 15.5, 31.1, 36, and 44.9 mg/g, respectively, at a salinity of 35 dS/m. These values were also found to be 0.9, 1.7, 2.8, and 3.8 at the salinity level of 5 dS/m. B3 had the best performance in absorbing HCO_3^- anion according to the results shown in Table 3. This means that at a salinity of 35 dS/m, it has absorbed 13.5 mg/g of HCO_3^-. However, the worst adsorption performance was related to the treatment with Sr, which not only did not play a role in the adsorption of HCO_3^- in all 4 salinity levels, but also caused a slight increase in HCO_3^- in the water. The problem may arise from the presence of organic substances in the composition of Sr. Because other adsorption treatments, which reduce the HCO_3^- of water, are all produced by the pyrolytic process, and all the organic substances in it are burned.

The adsorption capacities of Ca^{2+} and Mg^{2+} cations at a salinity level of 35 dS/m for the absorbents B1, B2, and B3 are distinctly noted, with values of 4.3, 5.2, and 3.7 mg/g for Ca^{2+} and 4.8, 6.2, and 2.8 mg/g for Mg^{2+}, respectively. The differences observed in adsorption capacities among these absorbents can be attributed to their distinct physicochemical properties, such as surface area, pore structure, and chemical composition. Notably, absorbent B2 exhibited the highest adsorption capacity for both Ca^{2+} and Mg^{2+}, with values reaching 5.2 mg/g and 6.2 mg/g, respectively. This enhanced performance may be linked to the presence of functional groups on the surface of B2 that facilitate ion exchange and adsorption. For instance, Wei-bin et al., (2024) highlighted that biochar with higher surface functional groups has improved ion retention capabilities, particularly for divalent cations like Ca^{2+} and Mg^{2+}.

According to the obtained results, the lowest amount of adsorption is related to K^+ cation. The amount of K^+ absorbed by Sr, B1, B2, and B3 adsorbents at the salinity level of 35 dS/m was found to be 0.8, 1.4, 1.7, and 2.5, respectively. Also, there was no significant difference in the amount of K^+ absorbed by all 4 adsorbents used at the salinity level of 5 dS/m. In general, the adsorption of K^+ by adsorbents is very low compared to other ions, so the amount of adsorption of Cl^- anion at a salinity level of 35 dS/m by B3 is about 56 times the amount of adsorption of K^+ at the same salinity level by B3.

By comparing the amount of adsorption of different ions at all salinity levels used, it can be concluded that the majority of the amount of ions absorbed by the adsorbents is related to Na^+ cations and Cl^- anions. For example, at a salinity level of 35 dS/m, the B3 adsorbent absorbed 140.7 mg/g of Cl^- anion and 91.5 mg/g of Na^+ cation, which represents 75% of all ions absorbed by this adsorbent. A higher gradient and greater access of the adsorbent to the salinity factor ions may account for the increase in adsorption by the adsorbent at higher salinities. The high ion concentration in the solution increases the possibility of cation and anion transfer to the adsorbent surface. The results of this part of the study are in complete agreement with the results of many other researchers as well (Shokrian et al., 2017 and 2020; Rostamian et al., 2015; Ghasemi et al., 2017 and 2018).

The desalination capacity (mg/g) of adsorbents at different salinities is illustrated in Fig. 4. The adsorption capacity of salinity ions in the lowest and highest state was found to be 5.6 and 308.6 mg/g, the lowest of which is related to the adsorption by Sr at the salinity level of 5 dS/m and the highest is related to the B3 was at a salinity level of 35 dS/m. Also, the adsorption capacity of the best adsorbent under study (B3) at salinity levels of 5, 10, 20, and 35 dS/m was obtained as 24.4, 57, 139.9, and 308.6 mg/g, equivalent to approximately 16%, 19%, 23%, and 29% of desalination respectively, which has a statistically significant difference with each other.

According to Table 3, the largest and smallest decreases in saline water EC occurred by B3 and Sr at salinity levels of 35 and 5 dS/m, respectively, which reduced the water salinity from 35 to 24.1 dS/m and from 5 to 4.83 dS/m, respectively, which in approximately 31 and 3% decreases, respectively. Generally, according to the results obtained, the best performance among the four adsorbents studied belongs to biochar prepared at 600 °C. The superiority of this absorber over other absorbers may be due to the higher specific surface area of this absorber compared to other absorbers and the larger volume of cavities of this absorber. This is because the larger specific surface area makes it possible for more ions to have access to the absorbent surface. Adsorption capacity is also largely dependent on the amount of access that the absorbed ions have to the internal surfaces of the absorbent cavities.

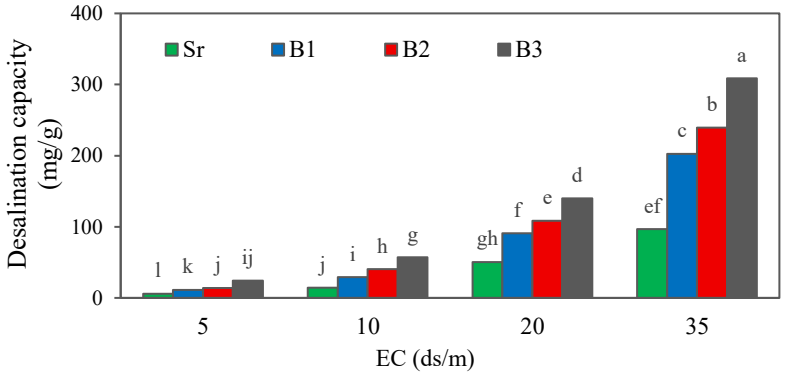

Fig. 4 Desalination capacity (mg/g) of adsorbents at different salinities

Means followed by the same letter are not significantly different at $P \leq 0.05$ according to LSD's test; Sr, Sesame residue; B1, Biochar-400; B2, Biochar-500; B3, Biochar-600.

3.4 Adsorption kinetics

To investigate the effect of contact time on the adsorption of saline ions, B3, which has the highest ability to absorb saline ions, was used at a salinity of 35 dS/m. Fig. 5 shows the effect of adsorbent contact time on the adsorption of cations and anions in 35 dS/m saline water. As can be seen in this figure,

the slope of the graph was high in the first 10 min of the experiment, indicating a high adsorption rate in the first 10 min. During this time, the adsorbent has absorbed approximately 66.1 mg/g of saline ions. This represents 21% of the total adsorption. Then, during the first 10 to 30 min of the experiment, the adsorption process was carried out at a higher rate. After this time, the adsorption process began to slow down. In this way, the adsorption process reached an equilibrium within 120 min after the start of the experiment. The reason for the high rate of adsorption of saline ions in the first 30 minutes of the experiment can be related to the abundance of absorbent surface ready and available for adsorption, which can quickly absorb the saline ions. However, over time, the absorbent surface available for adsorption decreases significantly (Hasan-Abadi et al., 2024).

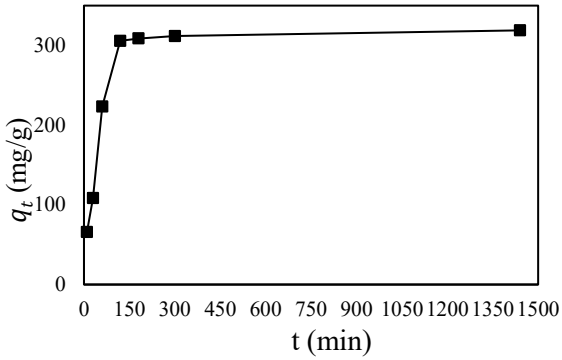

Fig. 5 Effect of contact time on the adsorption of saline ions for B3, Biochar-600

Table 4 Kinetic parameters for the adsorption of salinity ions of Biochar-600 (B3)

Model	Parameter	B3
Intra-particle diffusion	K_{dif}	18.915
	C	82.1
	R^2	0.8254
pseudo-first order	q_e(mg/g)	235.4
	$k_1(min^{-1})$	0.0134
	R^2	0.8203
pseudo-second order	q_e(mg/g)	285.1
	k_2 (g/mg min)	0.000009
	R^2	0.9773

In addition, for the estimation of the amount of adsorption, the pseudo-second-order kinetic model has a better performance than the other two models. According to the assumptions of the pseudo-second-order kinetic model, one of the effective processes in the adsorption of salinity factor ions is chemical adsorption. Many researchers have introduced the second-order kinetic model as the best kinetic model for the adsorption of ions or even heavy metals (Chen et al., 2023; Ghasemi et al., 2017 and 2018; Rahman et al., 2019).

3.5 Adsorption isotherms

After the adsorption process, the obtained data were fitted to the Langmuir and the Freundlich models, the results of which are presented in Table 5. Based on the obtained results, the correlation coefficients for the models based on Langmuir and Freundlich were obtained as 0.9995 and 0.9983, respectively. As a result, the Langmuir model was found to best agree with the experimental data. It can be concluded that, based on the assumptions of the Langmuir model, the adsorption of saline ions by the absorbent is of the single-layer type. The adsorption sites on the absorbent surface are uniform and homogeneous. It is fully consistent with the results of the adsorption isotherm, as in the previous research (Divband-Hafshejani et al., 2016; Farmani et al., 2020). In addition, the Freundlich model has a very high and acceptable level of agreement with the test data. According to this model, considering that the coefficient n is less than one, it can be concluded that the changes in the amount of absorbed ions were greater than the changes in the concentration of ions in the saline solution. In other words, as the salinity level increases, the use of adsorbents has been more effective in the adsorption of salinity factor ions.

Karami and Ghasemi (2020) also investigated the kinetics of phosphate adsorption using sugarcane bagasse biochar and calculated the time to reach equilibrium in the adsorption of phosphate ions to be 120 min. To better understand the dynamics of salt ion adsorption on adsorbents and to provide a predictive model to estimate the adsorption rate of absorbed ions during the process, adsorption kinetic models have also been studied. For this purpose, for the treatment of B3, the graph of adsorption changes was fitted with kinetic models of the Intra-particle diffusion, pseudo-first order, and pseudo-second-order at a salinity level of 35 dS/m, and the results are presented in Table 4. According to the results, the correlation coefficient for the B3 in the Intra-particle diffusion, pseudo-first-order, and pseudo-second-order was found to be 0.8254, 0.8203, and 0.9773, respectively.

Table 5 Isotherm parameters for the adsorption of salinity ions of Biochar-600 (B3)

Model	Parameter	B3
Langmuir	q_m(mg/g)	346.88
	k_1(L/mg)	3.6258
	R^2	0.9995
Freundlich	K_f(L/mg)	0.3013
	n	0.785
	R^2	0.9983
Temkin	A	0.00083
	B (kj/mol)	0.1167
	R^2	0.8733

4. Conclusion

In this study, to adsorb salinity ions from saline irrigation water, biochar adsorbents produced from sesame residue were applied. This study aimed to investigate the application of biochar adsorbents prepared from agricultural residues at different temperatures in the reduction and adsorption of salt ions. In this study, the characteristics of biochar prepared from sesame meal and its adsorption capacity were investigated. The results obtained from this section showed that:

1. Biochar adsorbents produced from sesame waste are effective in adsorbing salt ions from irrigation water, with the highest adsorption capacity (308.6 mg/g) observed for adsorbent B3 at a salinity of 35 dS/m.

2. Increasing pyrolysis temperature enhances the specific surface area and adsorption capacity of adsorbents but decreases the carbon-to-oxygen ratio and cation exchange capacity. Higher temperatures lead to the decomposition of oxygen-containing functional groups, resulting in a lower carbon-to-oxygen ratio and an increase in aromatic compounds. While cation exchange capacity diminishes, the larger surface area improves adsorption potential.

3. The presence of interfering ions can negatively affect the efficiency of the adsorbents, leading to a reduction in ion removal efficiency. The use of selective materials and pretreatment steps can help improve the performance of desalination systems.

4. The pseudo-second-order kinetic model and the Freundlich isotherm model showed the best fit to the experimental data, indicating the high potential of low-cost adsorbents for removing salt ions. However, non-linear estimation in kinetic and equilibrium models such as the Redlich-Peterson and Hill isotherms and the Boyd and Elovich kinetic models is also proposed to improve the results.

Despite the limitations of adsorption capacity and adsorbent stability, further research is needed in the areas of adsorbent improvement, modification methods, and the influence of other parameters such as solution pH and contact time. Generally, the salt adsorption capacity of adsorbents is always limited, and some research has been conducted on adsorbent stability and reuse. Nevertheless, the adsorption method is a cost-effective approach for salt adsorption or the removal of potentially toxic elements, and it still holds potential for further research and investigation in future studies. Low-cost adsorbents derived from agricultural waste, although capable of adsorbing salt or removing pollution from aquatic environments, also have limitations that have led to ongoing research. Research continues on determining the best adsorbent, methods for modifying them, their mechanisms of action, adsorbent stability, limited adsorption capacity. Given the advancement of science and the use of new adsorbents, perhaps only by modifying them can the adsorption capacity be increased to some extent, but in any case, the use of adsorbents cannot be permanent and sustainable. However, considering the necessity of water desalination, new methods or new adsorbents for this purpose are still being investigated and researched. It is suggested that future research should examine this important issue, as well as the effect of other parameters such as solution pH, contact time.

Statements and Declarations

Data availability

The authors confirm that the data supporting the findings of this study are available within the article.

Conflicts of interest

The author of this paper declared no conflict of interest regarding the authorship or publication of this paper.

Author contribution

M. Nouri-Shamsi and S. Soltani-Gerdefaramarzi: Material preparation, data collection, and analysis; M. Ghasemi and N. Yarami: Drafting the manuscript; All authors read and approved the final manuscript.

AI Use Declaration

This study did not incorporate artificial intelligence techniques; instead, all analyses and optimizations were conducted using conventional and widely accepted analytical methods.

References

Aghakhani, A., Mousavi, S. F., Mostafazadeh-Fard, B., Rostamian, R., & Seraji, M. (2011). Application of some combined adsorbents to remove salinity parameters from drainage water. *Desalination* 275(1-3): 217-223. https://doi.org/10.1016/j.desal.2011.03.003.

Ahmed, M. J., & Theydan, S.K. (2013). Microporous activated carbon from Siris seed pods by microwave-induced KOH activation for metronidazole adsorption. *Journal of Analytical and Applied Pyrolysis* 99: 101-109. https://doi.org/10.1016/j.jaap.2012.10.019.

Altintig, E., Arabaci, G., & Altundag, H. (2016). Preparation and characterization of the antibacterial efficiency of silver loaded activated carbon from corncobs. *Surface and Coatings Technology* 304: 63-67. https://doi.org/10.1016/j.surfcoat.2016.06.077.

Chen, S., Sun, L., Huang, Y., Yang, D., Zhou, M., & Zheng, D. (2023). Biochar-based interfacial evaporation materials derived from lignosulfonate for efficient desalination. *Carbon neutralization* https://doi.org/10.1002/cnl2.79.

Divband-Hafshejani, L., Mortazavi, P., Sabz Alipour, S., & Broomannasab, S. (2016). Isotherm and kinetics study of the adsorption of Chromium (VI) from aqueous solution by Zizyphus Spina-christi leaves Ash Nanoparticles. *Irrigation Sciences and Engineering* 39(4): 97-110. (In Persian). https://idj.iaid.ir/article_55273.html?lang=en.

Doula, M. K. (2007). Synthesis of a clinoptilolite–Fe system with high Cu sorption capacity. *Chemosphere* 67(4):731-740. http://dx.doi.org/10.1016/j.chemosphere.2006.10.072.

Farmani, B., Bodbodak, S., & Dadashi, S. (2021). Investigation of sorption isotherm models on remove ability sugar beet dilute molasses impurities using powdered activated carbon. *Journal of Food Science and Technology* 17(107):107-118. (In Persian). https://doi:10.52547/fsct.17.107.107.

Fatholahi, P., Salehzadeh, H., Hosseini, K., Wantala, K., Shivaraju, H.P., Jenkins, D., & Shahmoradi, B. (2023). Removal of erythromycin antibiotic from the aqueous media using magnetic graphene oxide nanoparticles. *Desalination and Water Treatment* 303:142-150. https://doi.org/S1944398624010804.

Ghasemi, M., Abedi Koupai, J., & Heidarpour, M. (2017). The effect of modified zeolite, activated carbon and peat with cationic surfactant and sodium hydroxide on removing anions from irrigation saline waters. *Desalination and Water Treatment* 92:196-204. https://doi: 10.5004/dwt.2017.21523.

Ghasemi, M., Abedi Koupai, J., & Heidarpour, M. (2018). Application of modified zeolite and modified peat in

removing salinity ions from irrigation saline waters. *Environmental engineering* 144(8): 04018066. https://doi:10.1061/(ASCE)EE.1943-7870.0001409.

Ghanbari Adivi, E., Mehrabinia, P., & Kermannezhad, J. (2020). Investigation of nitrate adsorption methods from contaminated waters using biochar. *Journal of Water and Sustainable Development* 7(1): 79-90. (In Persian). https://doi.org/10.22067/jwsd.v7i1.81367.

Hasan-Abadi, M., Soltani-Gerdefaramarzi, S., Ghasemi, M., & Azizian, A. (2024). Efficiency Investigation of biochar for desalination in the presence of copper ions. *Environment and Water Engineering* 10(4): 438-451. https://doi: 10.22034/ewe.2024.441749.1913.

Ho, Y.S., & McKay, G. (1999). Pseudo-second order model for sorption processes. *Process Biochemistry* 34(5): 451-465. https://doi.org/10.1016/S0032-9592(98)00112-5.

Hoveizavi, S., Tishehzan, P., & Hooshmand, A. (2024). Investigation of reducing the salinity of agricultural drainage water using cocopeat adsorbent. *Iranian Journal of Irrigation & Drainage 18*(3): 421-432. https://idj.iaid.ir/article_198967.html?lang=en.

Jellali, S., Khiari, B., Usman, M., Hamdi, H., Charabi, Y., & Jeguirim, M. (2021). Sludge-derived biochars: A review on the influence of synthesis conditions on pollutants removal efficiency from wastewaters. *Renewable and Sustainable Energy Reviews* 144:111068. https://doi.org/10.1016/j.rser.2021.111068.

Karami, S., & Ghasemi, R. (2020). Evaluation of Phosphate Sorption Kinetics by Sugar Cane Bagasse Biochar. *Water and Soil Science* 30(2): 47-58. https://water-soil.tabrizu.ac.ir/article_10884.html.

Lagergren, S. (1898). *Zur theorie der sogenannten adsorption geloster stoffe. Kungliga svenska vetenskapsakademiens*. Handlingar 24:1-39. https://www.scirp.org/reference/referencespapers?referenceid=1530542.

Li, A., Liu, H. L., Wang, H., Xu, H. B., Jin, L. F., Liu, J. L., & Hu, J. H. (2016). Effects of temperature and heating rate on the characteristics of molded bio-char. *Bio Resources*11(2): 3259-3274. https://doi.10.15376/biores.11.2.3259-3274.

Li, W. B., Deng, H. Y., Ye, Y., Zhou, S. N., Abbas, T., Ouyang, J. M., & Liu, W. (2022). Effect of pH on the adsorptive and cycling performance of amphoteric clay-loaded biochar. *Desalination and Water Treatment* 264: 111-120. https://doi: 10.5004/dwt.2022.28559.

Liang, L., Xi, F., Tan, W., Meng, X., Hu, B., & Wang, X. (2021). Review of organic and inorganic pollutants removal by biochar and biochar-based composites. *Biochar* 3: 255-281. https://doi.org/10.1007/s42773-021-00101-6.

Lin, L., Jiang, W., & Xu, P. (2017). Comparative study on pharmaceuticals adsorption in reclaimed water desalination concentrate using biochar: Impact of salts and organic matter. *Science of the Total Environment* 601: 857-864. https://doi.org/10.1016/j.scitotenv.2017.05.203.

Luo, Z., Yao, B., Yang, X., Wang, L., Xu, Z., Yan, X., & Zhou, Y. (2022). Novel insights into the adsorption of organic contaminants by biochar: a review. *Chemosphere* 287: 132113. https://doi: 10.1016/j.chemosphere.2021.132113.

Min, F., Zhang, M., Zhang, Y., Cao, Y., & Pan, W P. (2011). An experimental investigation into the gasification reactivity and structure of agricultural waste chars. *Journal of Analytical and Applied Pyrolysis* 92(1): 250-257. https://doi.org/10.1016/j.jaap.2011.06.005.

Priya, A.K., Gokulan, R., Vijayakumar, A., & Praveen, S. (2020). Biodecolorization of Remazol dyes using biochar derived from Ulva reticulata: isotherm, kinetics, desorption, and thermodynamic studies. *Desalination and Water Treatment* 200: 286-295. http://dx.doi.org/10.5004/dwt.2020.26098.

Qiu, B., Shao, Q., Shi, J., Yang, C., & Chu, H. (2022). Application of biochar for the adsorption of organic pollutants from wastewater: Modification strategies, mechanisms and challenges. *Separation and Purification Technology* 121925. https://doi.org/10.1016/j.seppur.2022.121925.

Rahman, M. S., Clark, M. W., Yee, L.m H., & Burton, E. D. (2019). Arsenic (V) sorption kinetics in long-term arsenic pesticide contaminated soils. *Applied Geochemistry* 111:104444. https://doi.org/10.1016/j.apgeochem.2019.104444.

Rostamian, R., Heidarpour, M., Mousavi, S. F., & Afyuni, M. (2015). Preparation, characterization and sodium sorption capability of rice husk carbonaceous adsorbents. *Fresenius Environmental Bulletin* 24(5): 1649-1658. https://www.researchgate.net/publication/292391877.

Rodriguez-Reinoso, F., Martin-Martinez, J. M., Molina-Sabio, M., Pérez-Lledó, I., & Prado-Burguete, C. (1985). A comparison of the porous texture of two CO_2 activated botanic materials. *Carbon* 23(1):19-24. https://doi.org/10.1016/0008-6223(85)90191-5.

Sahraei, M., Liaghat, A., & Nazi Ghameshlou, A. (2022). Investigating the Effect of Using Iranian Zeolite and Bentonite in Desalination. *Journal of Water and Wastewater; Ab va Fazilab* 32(6): 58-66. https://doi: 10.22093/wwj.2021.273711.3117.

Salehzadeh, H., Shahmoradi, B., Maleki, A., Nikkhoo, B., Rahimi, B., Rezaee, M., Mohammadi, E., Shivaraju, H. P., Ren, G., Wantala, K., & Choi, H. J. (2024). Magnetically separable BiZnO/Fe3O4 nanocomposites and their application for degradation of 2, 4-dichlorophenoxyacetic acid pesticide. *Materials Today Sustainability* 28: 100962. https://doi.org/abs/pii/S2589234724002987.

Shokrian, F., Solaimani, K., Nematzadeh, G., & Biparva, P. (2017). Feasibility of water salinity reduction by rice husk and shell as bio sorbent. *Journal of Irrigation and Water Engineering* 7(3): 93-106. (In Persian). https://www.waterjournal.ir/article_74061.html.

Shokrian, F., Solaimani, K., Nematzadeh, G., & Biparva, P. (2020). Comparative Investigation of Bio and Mineral

Absorbents on Water Salinity Reduction. *Journal of Environmental Science and Technology* 22(4): 55-66. (In Persian). https://doi: 10.22034/jest.2018.24400.3353.

Simonin, J. P., & Bouté, J. (2016). Intraparticle diffusion-adsorption model to describe liquid/solid adsorption kinetics. *Revista mexicana de ingeniería química* 15(1):161-173. https://www.scielo.org.mx/scielo.php?script=sci_arttext&pid=S1665-27382016000100161.

Singh, B., Singh, B. P., & Cowie, A L. (2010). Characterization and evaluation of biochars for their application as a soil amendment. *Soil Research* 48(7): 516-525. http://dx.doi.org/10.1071/SR10058.

Wei-bin, Z. H. A. O., Song, W. A. N. G., Ling-ling, L. I. U., Jiang, X. I. A. O., Shu-feng, W. A. N. G., Li, T. A. N. G., & Guang-cai, C. H. E. N. (2024). Effect of biochar amendment on saline-alkaline soil amelioration and plant growth: A literature review. *Chinese Journal of Soil Science* 55(2): 551-561. https://doi: 10.19336/j.cnki.trtb.2022090803.

Yang, H., Ye, S., Zeng, Z., Zeng, G., Tan, X., Xiao, R., & Xu, F. (2020). Utilization of biochar for resource recovery from water: *A review. Chemical Engineering Journal* 397: 125502. http://dx.doi.org/10.1016/j.cej.2020.125502.

Younis, S. A., El-Salamony, R. A., Tsang, Y. F., & Kim, K. H. (2020). Use of rice straw-based biochar for batch sorption of barium/strontium from saline water: Protection against scale formation in petroleum/desalination industries. *Journal of Cleaner Production* 250: 119442. http://dx.doi.org/10.1016/j.jclepro.2019.119442.